



Long-term fate of rapidly eroding carbon stock soil profiles in coastal wetlands

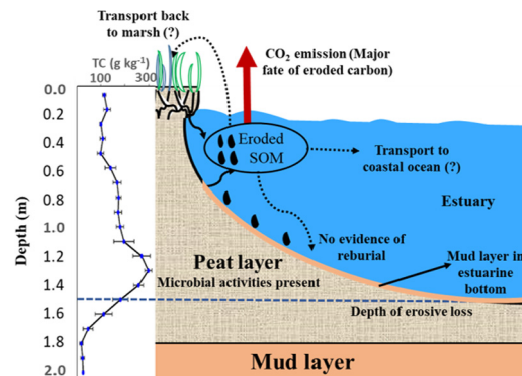
Yadav Sapkota, John R. White*

Wetland and Aquatic Biogeochemistry Laboratory, Department of Oceanography and Coastal Sciences, Louisiana State University, Baton Rouge, LA, United States of America

HIGHLIGHTS

- Total carbon and carbon density increased with depth up to 1.3 m.
- Enzyme and microbial activities present at all depths.
- Eroded carbon is highly susceptible to mineralization in estuaries.
- Coastlines projecting high sea-level rise may lose large amounts of stored carbon.

GRAPHICAL ABSTRACT



ARTICLE INFO

Article history:

Received 22 June 2020

Received in revised form 20 August 2020

Accepted 21 August 2020

Available online 26 August 2020

Editor: Jay Gan

Keywords:

Blue carbon

Decomposition

CO₂ emission

Marsh edge erosion

Sea-level rise

Climate change

ABSTRACT

Marsh edge erosion is one of the major causes of land and associated carbon loss in wetland-dominated coastlines. Assessing carbon stocks and understanding fate of eroding carbon is an essential component of wetland carbon budget. This study aims to understand the vertical soil carbon profile of an eroding marsh and potential mineralization of carbon in estuaries. Eleven soil cores (~2 m deep) were collected from the edge of four highly eroding marsh sites and three cores from the estuarine bottom (~50 cm deep). Cores were sectioned into 10-cm intervals and analyzed for total, labile and refractory carbon, carbon density, select enzyme and microbial activities, and organic and inorganic phosphorus forms. The total carbon, labile carbon, and carbon density increased with depth at all sites. The carbon density at 1–1.5 m deep ($0.04 \pm 0.003 \text{ g cm}^{-3}$) was significantly higher ($p < 0.0001$) than the top 1 m soil ($0.032 \pm 0.002 \text{ g cm}^{-3}$), indicating the need for considering deeper carbon profile for blue carbon stock assessment. The age of the carbon at the estuarine bottom was 388 ± 84 years before present (ybp) indicating the recently eroded wetland carbon is not reburied in the estuary. Significant anaerobic microbial activity was present at all the soil depths suggesting high potential of mineralization of eroded carbon in the aerobic estuarine water. The coastlines experiencing high relative sea-level rise at present or coastlines that are projecting high sea-level rise in the near future are susceptible to losing an enormous amount of previously sequestered carbon over a relatively short period of time.

© 2020 Elsevier B.V. All rights reserved.

1. Introduction

Coastal wetlands are one of the most productive ecosystems on the earth. These wetlands provide a variety of ecosystem services and are increasingly recognized for atmospheric carbon sequestration

* Corresponding author.

E-mail address: jrwhite@lsu.edu (J.R. White).

(Chmura et al., 2003; Reddy and DeLaune, 2008; Murray et al., 2011). The global interest in coastal wetlands for carbon sequestration and storage is rising as the atmospheric concentration of the CO₂ is setting a new high record every year (NOAA, 2019). The top one-meter of salt marsh soil has been estimated to contain approximately 917 t CO₂ e ha⁻¹ with annual carbon sequestration of 8.0 ± 8.5 t CO₂ e ha⁻¹ (Murray et al., 2011).

However, coastal wetland acreage is shrinking due to a number of factors including sea-level rise, local subsidence, wind wave driven edge erosion, extreme weather events, and anthropogenic influences including hydrologic alterations and coastal developments (DeLaune and White, 2012). The degradation and loss of coastal ecosystems not only reduces the potential area for additional carbon sequestration but can also release a large amount of carbon that has been previously sequestered over decades to centuries (Sierra et al., 2018). Globally, almost 50% of wetlands have been lost in 20th century (Davidson, 2014). Marsh edge erosion is one of the critical drivers of land loss along wetland dominated coastlines that results in the transport and release of the stored carbon into adjacent estuaries (Wilson and Allison, 2008; Sapkota and White, 2019). For example, coastal Louisiana, USA has lost almost 25% (~5000 km²) of its coastal wetlands since 1932 CE with the current wetland loss rate of approximately 57.5 km² y⁻¹ (Couvillion et al., 2017). The marsh edge erosion is the major cause of this wetland loss influenced by high relative sea-level rise (13 mm y⁻¹; Jankowski et al., 2017), subsidence, and limited sediment supply for vertical accretion (Nyman et al., 1994; Wilson and Allison, 2008; Blum and Roberts, 2009; Morton et al., 2009).

Marsh edge erosion, due to undercutting by waves, results in the initial collapse of a column of soil approximately 40 cm in height, followed by submergence (Sapkota and White, 2019; Valentine and Mariotti, 2019). Wave scour then continuously dislodges submerged peat material into the estuary water until the bottom of the estuary achieves an equilibrium bathymetric profile dependent upon wave climate (Wilson and Allison, 2008). The bedload shear created by wind waves further degrades the transported and released (referred to 'eroded' hereafter) material, exposing the organic matter to the oxygenated bay water. Several studies have noted that the long-term fate of this eroded SOM has not been previously well understood (Mack et al., 2012; Holmquist et al., 2018; Needelman et al., 2018; Macreadie et al., 2019). Some recent studies have shown that a significant fraction of the eroded carbon upon exposure to well mixed aerobic water of shallow estuary becomes mineralized to CO₂ and emitted back in to the atmosphere (DeLaune and White, 2012; Steinmuller et al., 2019; Steinmuller and Chambers, 2019; Haywood et al., 2020). Some studies indicate that the significant portion of this eroded carbon may get reburied in the estuarine bottom (Li et al., 2009; Macreadie et al., 2013), transported to the coastal ocean (Bianchi et al., 2008; Li et al., 2009) or transported back to the marsh platform by wind waves (Hopkinson et al., 2018; Mariotti et al., 2020) (Fig. 1).

The long-term fate of the eroded SOM may depend on the molecular complexity of the SOM, bioavailable pool of nutrients, and associated microbial activity in eroded marsh edge and submerged soil. The relative complexity and hence recalcitrance of the organic matter has been shown to increase with depth, owing to the presence of greater high-molecular-weight refractory organic matter and lower microbial activities at depths (Webster and Benfield, 1986; Schipper and Reddy, 1995; Mendelsohn et al., 1999). The degradation is also reduced by the low availability of alternate electron acceptors in the anaerobic environment (Reddy and DeLaune, 2008). The highly labile fraction of organic matter is preferentially degraded at the surface before burial resulting in the storage of refractory organic matter at depths over time (DeBusk and Reddy, 1998; Reddy and DeLaune, 2008; Bianchi and Canuel, 2011). However, a few recent studies have shown increased degradability of organic material at depth challenging the established concept of the presence of less degradable SOM at depths (Schmidt et al., 2011; Steinmuller et al., 2019; Steinmuller and Chambers, 2019;

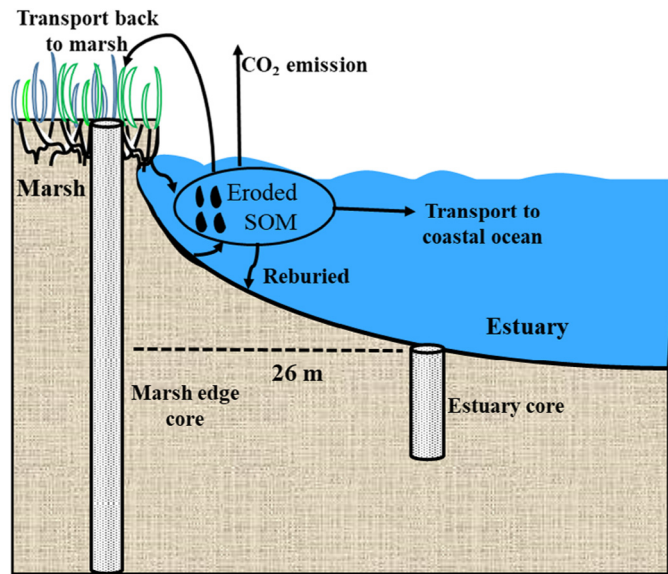


Fig. 1. Conceptual diagram of marsh edge and estuary showing the potential fate of eroded soil organic matter (SOM) and soil sampling points. Marsh edge cores (~2 m deep) were collected 1 m in to the marsh from the edge. The estuary bottom cores (~0.5 m deep) were collected 25 m in to the estuary from the edge of the marsh (Yadav Island). The horizontal and vertical scale in the diagram is different.

Haywood et al., 2020). This finding may be related to changes in depositional environment and related macrophyte species shifts from fresh to salt marshes in response to sea-level rise, which changes the nature of carbon deposited (DeLaune, 1986).

The majority of the studies on wetland soil organic matter are based on the top 30 to 50 cm soil (Choi and Wang, 2004; Wood et al., 2017; Levine et al., 2017; Vaccare et al., 2019; Vaughn et al., 2020) assuming the majority of the microbial activity occurs within the surficial soil (Reddy and DeLaune, 2008) with a few recent studies looking at microbial and enzyme activities up to depth of 1–1.5 m (Steinmuller et al., 2019; Steinmuller and Chambers, 2019; Haywood et al., 2020). These recent studies also have shown increased carbon content with depth. Nahlik and Fennessy (2016) have shown that almost 65% of the soil carbon is present between the depths of 30–120 cm in the wetlands of the continental US. However, the blue carbon offset methodologies generally consider top one-meter depth during carbon stock assessment (Mack et al., 2012; Howard et al., 2014; Emmer et al., 2015; Sapkota and White, 2020). Consequently, the top one-meter wetland soil has been a focus of the blue carbon stock study and reporting. The larger synthesis and meta-analyses studies on wetland soil carbon stock and density are constrained to top one-meter depth and haven't considered carbon profiles deeper than 1 m (Chmura et al., 2003; Choi and Wang, 2004; Hinson et al., 2019). The SOM deposits in deltaic coastal wetland may extend to a few meters in thickness indicating the need for a greater number of deep (> 1 m) carbon profile studies for carbon stock assessment (Howard et al., 2014; Nyman, 2014). In addition, the current focus is on the quantification of blue carbon stock and sequestration potential in coastal ecosystems to make predictions going forward. However, the relative permanence of preservation and storage of these deeper carbon stocks depend on the biogeochemical properties of SOM and environmental factors, which are not extensively studied.

The goal of this study was to understand the potential mineralization of marsh edge SOM in the coastal estuaries with depth. Here we looked at the molecular-complexity, available nutrient pools and microbial activity in marsh edge (~2 m deep) and submerged soil to understand changes to potential SOM degradability. Understanding the potential degradability of eroding and submerged SOM is helpful in predicting the long-term fate of eroded carbon in the coastal estuaries. We

hypothesize that the total carbon, bioavailable nutrients, labile pool of carbon and microbial activity would decrease with depth.

2. Methods

2.1. Study site

Barataria Basin, an estuary in southeast Louisiana, USA, was selected as a study site (Fig. 2). Barataria Bay wetlands are experiencing some of the highest coastal erosion rates in the Continental US. The coastal basin is disconnected from the Mississippi River through a continuous system of levees and therefore has limited sediment supply. Continuous erosion and submergence due to rising sea-level with no new land building have resulted in rapid wetland loss in this area. The entire basin has lost approximately 1172 km² of coastal land in the period between 1932 and 2016 with a mean loss rate of approximately 13.3 km² y⁻¹ (Couvillion et al., 2017). The marshes in the northern part of the Barataria Bay range from brackish to salt marshes with the dominant vegetation of *Spartina patens* and *Spartina alterniflora*. Barataria Bay is a micro-tidal system with a diurnal tidal regime (Georgiou et al., 2005).

Two eroding islands vegetated with *Spartina alterniflora* were selected for this study (Fig. 2). Marsh edge erosion rates were monitored at these islands for three years and the mean edge erosion rate was 1.42 ± 0.2 m y⁻¹ (Sapkota and White, 2019). Yadav island has three sampling sites with shorelines facing north, west and south sides. Ben's island is a site with an east facing shoreline. Altogether, we had four sampling sites with the shorelines facing four different cardinal directions with variable erosion rates.

2.2. Soil sampling

Eleven soil cores (~2 m deep) were collected 1 m inland from the marsh edge of four different sites; nine cores from Yadav island and

two cores from Ben's island. A polycarbonate core tube (2.6 m \times 7.6 cm diameter) was used to extract soil samples via the push core method. In addition, triplicate cores (50 cm deep) were collected using a piston corer from the bottom of the estuary, at 25 m from the edge of Yadav island at a water depth of 1 m. Soils were extruded in the field, sectioned into the 10-cm intervals and placed and sealed in zip-lock bags. Samples were stored on ice, immediately transported to Louisiana State University (LSU), and stored at 4 °C until analysis.

2.3. Laboratory analysis

All the laboratory analyses except radiocarbon dating of the carbon were performed within Wetland and Aquatic Biogeochemistry Laboratory, Louisiana State University. All the analyses were subject to quality assurance and control (QA/QC) measures including the repeats, blanks, spikes where applicable, and external quality control standards. The recovery of the standards between 90% to 110% were accepted. The radiocarbon dating of the soil carbon was performed by a well-known radiocarbon analysis laboratory (Beta Analytics LLC, Miami, FL, USA).

2.3.1. Soil physiochemical properties

Each sample was initially weighed, homogenized, and subsampled for further analysis. Subsamples were analyzed for soil physiochemical properties including moisture content, bulk density, percent organic matter (% OM), total carbon (TC), total nitrogen (TN) and total phosphorus (TP). A weighed 30–40 g aliquot of moist soil was dried at 60 °C in a forced air oven until a constant weight was achieved to determine gravimetric moisture content. The dry bulk density of each sample was determined by calculating the total dry weight of the sample and then dividing by the volume of the 10 cm section of the core (384.85 cm³). The dried samples were ground into fine particles using a mortar and pestle. TC and TN were determined from the ground sub-sample using an elemental combustion system (Costech Analytical

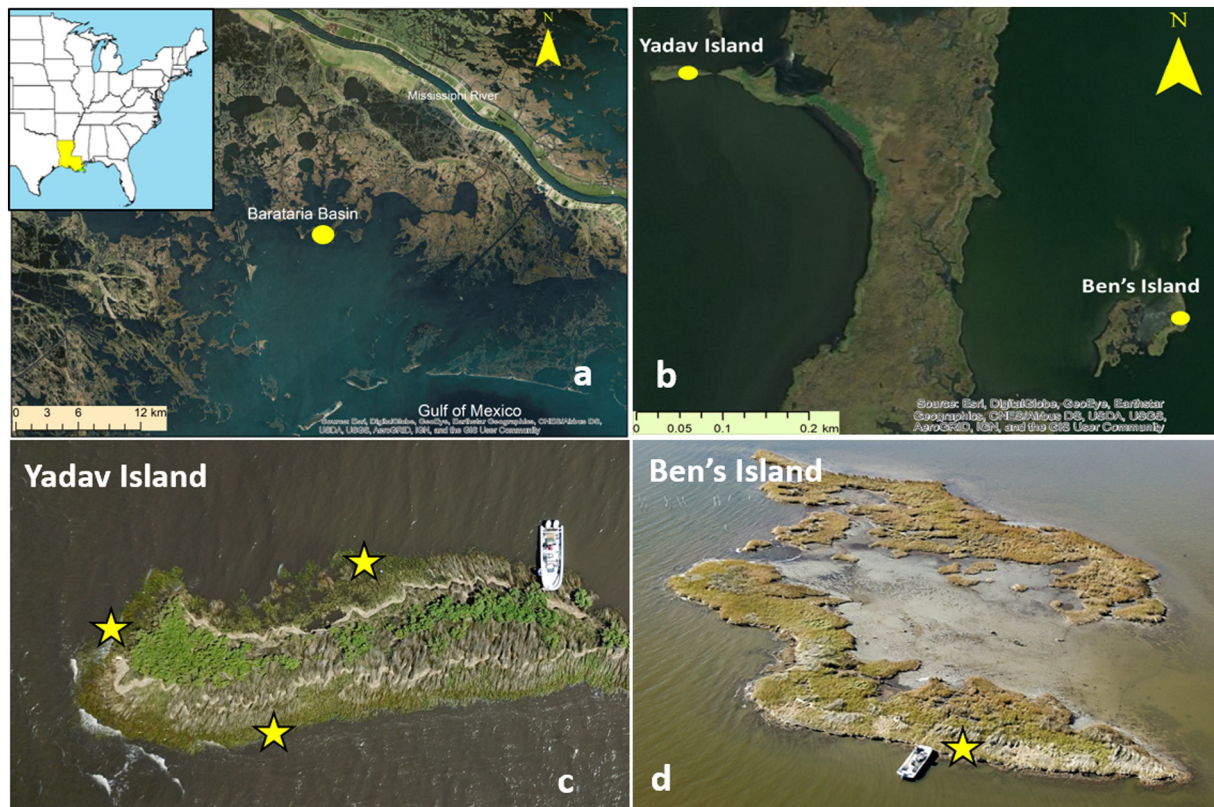


Fig. 2. Map of study sites. a) Location of the Louisiana in the US and the Barataria Basin in Louisiana, b) Location of Yadav and Ben's island in Barataria Basin, c) Yadav island with three sampling sites, and d) Ben's island with a sampling site. Figure c and d (drone photos) courtesy of Eddie Weeks.

Technologies, Valencia, CA). The volumetric concentration of the TC (g cm^{-3} ; carbon density) was determined by dividing the amount of TC in 10 cm section of the core by the volume of the 10 cm section of the core. The % OM was determined by the loss on ignition (LOI) technique following Sparks (1996). 0.2–0.5 g subsamples were weighed in 50 mL glass beakers and burned in a muffle furnace at 550 °C for 4 h. The ashed weight of the sample was divided by the pre-ash weight to determine weight % OM. Total phosphorus was determined by acid digesting ashed samples following Andersen (1976) and analyzed colorimetrically using a SEAL AQ2 Automated Discrete Analyzer (SEAL Analytical Inc., Mequon, Wisconsin) with a detection limit of 0.002 mg P L^{-1} (USEPA, 1993).

Total inorganic phosphorus (TIP) was extracted from dried and ground samples following Richardson and Reddy (2013). Samples of 0.3–0.5 g were weighed in centrifuge tubes, and equilibrated with 25 mL of 1 M HCl for 3 h in a longitudinal shaker, centrifuged for 10 min @ 5000g and vacuum filtered through a 0.45 μm filter. The filtered solution was analyzed for TIP colorimetrically using a SEAL AQ2 Automated Discrete Analyzer (SEAL Analytical Inc., Mequon, Wisconsin) with a detection limit of 0.002 mg P L^{-1} (USEPA, 1993). Total organic phosphorus (TOP) was determined by difference of TIP from TP.

2.3.2. Carbon fractionation

The molecular complexity of the organic matter was determined from dried and ground soil subsamples through a H_2SO_4 extraction following Rovira and Vallejo (2002) and Oades et al. (1970) with modifications by Steimuller and Chambers (2019). The organic matter was separated into two groups-1) Labile pool of carbon (LPC) consisting of plant or microbially derived non-cellulosic polysaccharides, hemicellulose, and cellulose and 2) Refractory pool of carbon (RPC) consisting of kason lignin, fats, waxes, resins, and suberins (Rovira and Vallejo, 2002). To extract LPC, 2 mL of 26 N H_2SO_4 was added to a flask containing ~0.5 g of dried and ground soil. The solution was shaken in an orbital shaker at 100 rpm for 14 h and diluted to a concentration of 2 N H_2SO_4 by adding 26 mL nanopure water. The resulting solution was heated at 105 °C for 3 h, allowed to cool, filtered through Watman #41 filters and then diluted to a final volume of 50 mL. The concentration of LPC was determined using a Shimadzu TOC-V (Shimadzu, Kyoto, Japan) following Qualls (2013). The amount of RPC was calculated by deducting the LPC from the TC content of the soil.

2.3.3. Enzyme activity

Extracellular enzyme assays were performed within 48 h of the sample collection to determine the activity of β -glucosidase, β -xylosidase, and alkaline phosphatase. Soils from the triplicate marsh (Yadav Island) and estuary cores were analyzed. Marsh soils were analyzed on a 30 cm depth interval from the surface to the depth of 160–170 cm. The estuary cores were analyzed on alternate depths from the surface to 40–50 cm depth. Enzyme Assays were performed using fluorescent substrate 4-methylumbelliflone (MUF) for standardization and fluorescently labeled MUF-specific substrates (German et al., 2011). A soil slurry was created adding ~1 g of moist soil to 40 mL of deionized water and shaken on an orbital shaker for 1 h at 25 °C and 150 rpm. Fluorescence was measured at excitation/emission wavelengths 360/460 nm on a BioTek Synergy HTX (BioTek Instruments, Inc., Winooski, VT, USA) both immediately after substrate and sample were added and 24 h later to determine a rate of enzyme activity.

2.3.4. Potentially mineralizable nitrogen (PMN) and phosphorus (PMP)

Soils from triplicate marsh and estuary cores (same depth interval as enzyme activity) were incubated following White and Reddy (2000) to determine PMN and PMP rates. Four sets of samples were assigned a time of 0, 2, 5, and 10 days of incubation at 40 °C. For zero-day sample, field-moist soil (~5 g) was weighed into 40 mL centrifuge tubes with 25 mL of 2 M KCl added, shaken on an orbital shaker at 150 rpm and 25 °C for 30 min, and centrifuged at 4000g for 10 min at 10 °C. Each

sample was vacuum-filtered through 0.45 μm membrane filters, acidified to a pH < 2 with sulfuric acid, and stored at 4 °C. For 2, 5, and 10-days samples, field moist soil (~10 g) was weighed in to a 40 mL glass serum bottle and sealed with rubber septa and aluminum crimp. Head space was evacuated until ~75 k Pa, purged with N_2 gas for 10 min, and 15 mL of N_2 purged filtered site water was then added through a syringe to create a slurry. The serum bottles were incubated at 40 °C and shaking at 120 rpm in an Incubated Shaker (IS-971, Jeio Tech Lab Companion, Daejeon, Korea). On the designated day, samples were removed from the incubator, added with 25 mL of 2 M KCl using a syringe, and placed in a shaker for 30 min. Then samples were transferred to 40 mL centrifuge tubes and centrifuged at 4000g for 10 min at 10 °C. Each sample was vacuum-filtered through 0.45 μm membrane filters, acidified to a pH < 2 with ultrapure concentrated sulfuric acid, and stored at 4 °C. Each sample was analyzed for extractable ammonium (Ext. NH_4^+) and soluble reactive phosphorus (Ext. SRP) colorimetrically using a SEAL AQ300 Automated Discrete Analyzer (SEAL Analytical Inc., Mequon, Wisconsin) with a detection limit of 0.01 mg N L^{-1} and 0.002 mg P L^{-1} (USEPA, 1993). The Ext. NH_4^+ and Ext. SRP concentrations at zero-day incubation represent an initial concentration of bioavailable N and P in each sample. The PMN and PMP rates were determined by regressing Ext. NH_4^+ and Ext. SRP concentrations over incubation time.

2.3.5. ^{14}C dating of the organic matter

Two piston cores were taken from the bottom of the estuary adjacent to the west side of Yadav Island. The samples were taken at 34 m and 58 m away from the edge of the marsh. The depth of water in estuary was 87 cm at both sampling points. The bottom surface of the estuary was 102 cm below the surface of the marsh. We discarded top 3 cm layer of the core to remove shell hash and the 10 cm sections below this top 3 cm layer were sent to Beta Analytics LLC, Miami, FL for radiocarbon dating on the decayed plant materials. Samples were pretreated with acid/alkali/acid and decayed plant materials were isolated for ^{14}C dating. The radiocarbon dating was performed on accelerator mass spectrometry (AMS). The stable carbon isotope ($\delta^{13}\text{C}$) values were measured separately in an isotope ratio mass spectrometer. The AMS results were corrected for total fractionation effects using $\delta^{13}\text{C}$ values. The conventional radiocarbon age (BP = 1950; Flint and Deevey, 1962) was calibrated to calendar years (cal CE) using BetaCal 3.21 that utilize INTCAL13 database (Reimer et al., 2013) and high probability density range method (HPD) (Bronk Ramsey, 2009). The calibrated radiocarbon age (ybp) was then calculated and reported as mean \pm standard error.

2.4. Statistical analysis

Statistical analyses were performed using R (Version 3.5.3; R Foundation for Statistical Computing, Vienna, Austria) in RStudio (Version 1.1.456; RStudio Inc., Boston, MA, USA). All the soil physiochemical data except carbon density were log-transformed to achieve the condition of normality. An ANOVA was run on soil physiochemical data with site, depth, and interaction as fixed effects. The multiple comparisons were done using the Tukey HSD method and Bonferroni correction was applied to the significance level (alpha value = 0.002). The soil physiochemical properties for marsh edge and submerged soil were compared using Welch two-sample *t*-test. The plots were prepared as means (\pm standard error) by soil depth using ggplot2 package in R (Wickham, 2016). The correlation coefficients between soil properties were obtained from JMP (SAS Institute, Cary, NC, USA).

3. Results

3.1. Soil physiochemical properties

The eroding marsh edge soil physiochemical properties including bulk density, % OM, TC, TN, and TP significantly varied with depth but

not with site (Supplementary Table 1). Mean bulk density of soil is almost constant up to the depth of 40–50 cm ($0.30 \pm 0.03 \text{ g cm}^{-3}$), gradually decreased to $0.15 \pm 0.01 \text{ g cm}^{-3}$ up to the depth of 120–130 cm, and then continuously increased to $0.80 \pm 0.07 \text{ g cm}^{-3}$ at the depth of 170–180 cm (Supplementary Fig. 1a). The % OM and TN increased up to the depth of 120–130 cm and then decreased (Supplementary Fig. 1b, c). Total carbon content increased from $99.85 \pm 13.27 \text{ g kg}^{-1}$ soil at the depth of 40–50 cm to $297.16 \pm 14.38 \text{ g kg}^{-1}$ at the depth of 120–130 cm and then gradually decreased to $19.08 \pm 6.46 \text{ g kg}^{-1}$ at the depth of 170–180 cm (Fig. 3a). The carbon density followed the trend of TC on a concentration basis (g kg^{-1}) with the average of $0.030 \pm 0.002 \text{ g cm}^{-3}$ on top 2 m deep soil (Fig. 3b). The carbon density between the depth of 1–1.5 m ($0.04 \pm 0.003 \text{ g cm}^{-3}$) was significantly higher ($p < 0.0001$) than top 1 m soil ($0.032 \pm 0.002 \text{ g cm}^{-3}$) and between the depth of 1.5–2 m ($0.019 \pm 0.004 \text{ g cm}^{-3}$). The soil physicochemical properties including bulk density, % OM, TC, and TN were correlated with each other (Supplementary Table 2).

During sampling, the estuary bottom was 1 m below the surface of the marsh. Therefore, we compared the 0–50 cm interval of the submerged estuary bottom soil with 100–150 cm depth of the adjacent marsh edge soil. The submerged soil physicochemical properties including bulk density, % OM, TC, TN, and TP significantly varied with depth ($p < 0.0001$) and followed the trend of marsh edge soil (Supplementary Fig. 2). The submerged soil % OM was significantly lower ($p < 0.0001$) at the depth of 0–20 cm compared to marsh edge soil. The % OM at other depths, bulk density, TC, TN, and TP were not significantly different between marsh edge and submerged soil.

3.2. Carbon fractionation

The LPC in marsh edge soil decreased from the surface ($24.22 \pm 1.69 \text{ g kg}^{-1}$) to the depth of 40–50 cm ($17.9 \pm 2.11 \text{ g kg}^{-1}$), gradually increased up to the depth of 120–130 cm ($47.31 \pm 2.41 \text{ g kg}^{-1}$), then decreased to $3.04 \pm 0.75 \text{ g kg}^{-1}$ at the depth of 170–180 cm (Fig. 3c). On the percentage basis, the LPC consists of almost 13.7% to 21.1% of the TC and generally slightly decreased with depth. The proportion

of LPC and RPC slightly decreased from the surface (0.27) to the depth of 60–70 cm (0.16). At the depth of 80–90 cm, the proportion increased to 0.24 and remains almost constant up to the depth of 170–180 cm. Both the LPC and RPC carbon were significantly correlated with bulk density, % OM, TC, TN, TIP, and TOP (Supplementary Table 2). In submerged estuary bottom soil, the LPC was similar in concentration to the marsh edge soil and followed the trend of marsh edge soil (Supplementary Fig. 2).

3.3. Phosphorus fractionation

Both TOP and TIP were significantly affected by depth (Supplementary Table 1). The TOP was significantly higher from the surface to the depth of 140–150 cm except at the depth of the 40–50 cm which could potentially be associated with storm event or river influence (Spera et al., 2020). At the depth of 150–160 cm both TOP and TIP had similar concentration beyond which the TIP was significantly higher (Fig. 4). The higher TIP concentration beyond 160 cm depth is the indication of deltaic processes of Mississippi River (Spera et al., 2020). The TIP and TOP were correlated with bulk density, % OM, TC, TN, LPC, and RPC.

3.4. Soil biogeochemical properties

Extracellular enzyme activity, PMN, and PMP analyses were performed on select depths of marsh edge soil as proxies for microbial activity. The extracellular enzyme activities including β -glucosidase, β -xylosidase, and alkaline phosphatase activity were present at all the depth of the soil analyzed. Generally, these enzyme activities variably increased from the surface to the depth of 120–130 cm and then decreased (Fig. 5). The β -glucosidase, β -xylosidase, and alkaline phosphatase activity were significantly correlated with each other (Supplementary Table 3). Likewise, these enzyme activities were correlated with % OM, TC, TN, and LPC (Supplementary Table 3).

The extractable NH_4^+ increased from the surface ($2.29 \pm 0.8 \text{ mg kg}^{-1}$) to the depth of 120–130 cm ($38.67 \pm 1.42 \text{ mg kg}^{-1}$) and then decreased

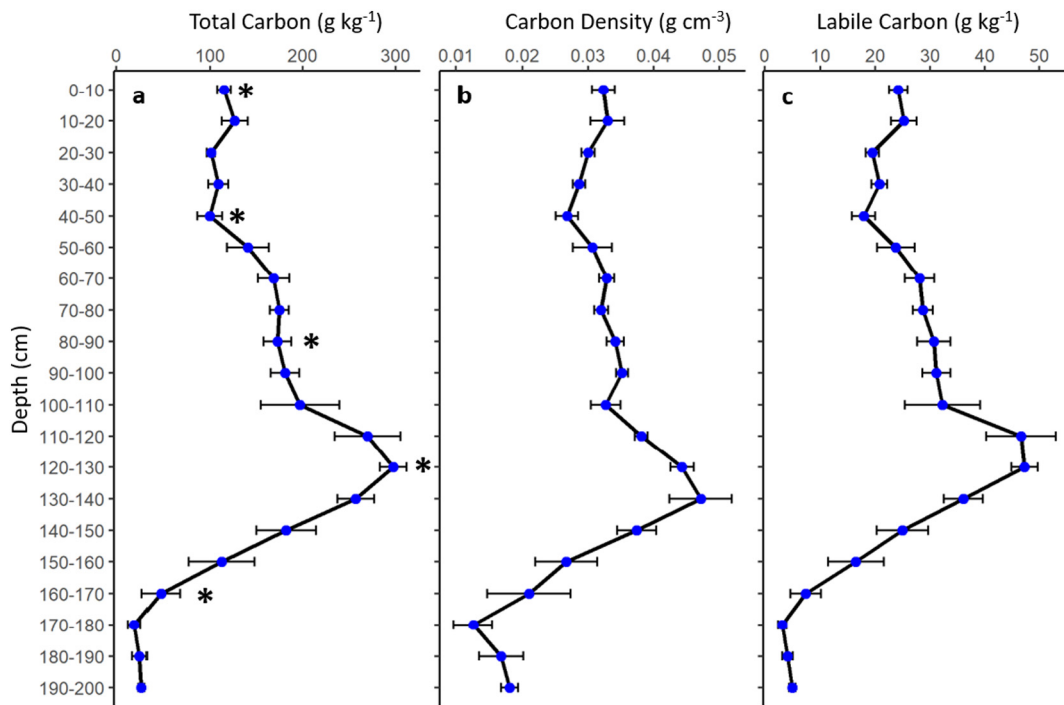


Fig. 3. Vertical carbon profile of eroding marsh edge soil. a) Total carbon, b) carbon density and, c) labile carbon. Total C and labile C expressed as gram C per kilogram of dry soil. The data expressed as mean \pm standard error ($n = 8$). *Depth intervals at which soil biogeochemical properties were analyzed.

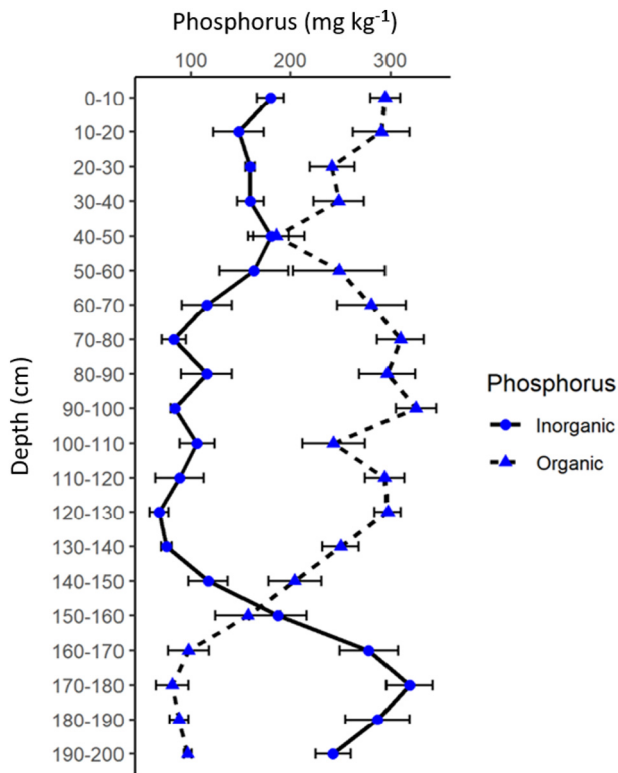


Fig. 4. Vertical profile of eroding marsh edge soil organic and inorganic form of the Phosphorus. The data expressed as mean \pm standard error ($n = 8$).

(Fig. 6). The soluble reactive phosphorus (SRP) increased from the surface ($0.36 \pm 0.18 \text{ mg kg}^{-1}$) to the depth of 80–90 cm ($2.45 \pm 1.43 \text{ mg kg}^{-1}$) and then decreased. The PMN rate decreased from the surface ($25.05 \pm 4.64 \text{ mg kg}^{-1} \text{ d}^{-1}$) to the depth of 80–90 cm ($9.44 \pm 1.2 \text{ mg kg}^{-1} \text{ d}^{-1}$), slightly increased at the depth of 120–130 cm ($14.72 \pm 0.67 \text{ mg kg}^{-1} \text{ d}^{-1}$) and then decreased. The PMP rate also decreased from the surface ($1.19 \pm 0.5 \text{ mg kg}^{-1} \text{ d}^{-1}$) to the depth of 160–170 cm ($0.08 \pm 0.02 \text{ mg kg}^{-1} \text{ d}^{-1}$) except being slightly increased at the depth of 120–130 cm ($1.02 \pm 0.09 \text{ mg kg}^{-1} \text{ d}^{-1}$) (Fig. 6). The PMN and PMP rates were correlated with each other but were not correlated with % OM and TC content of the marsh edge soil (Supplementary Table 3).

In the submerged soil, a substantial rate of PMN, PMP and extracellular enzyme activities was observed across the depth of the soil

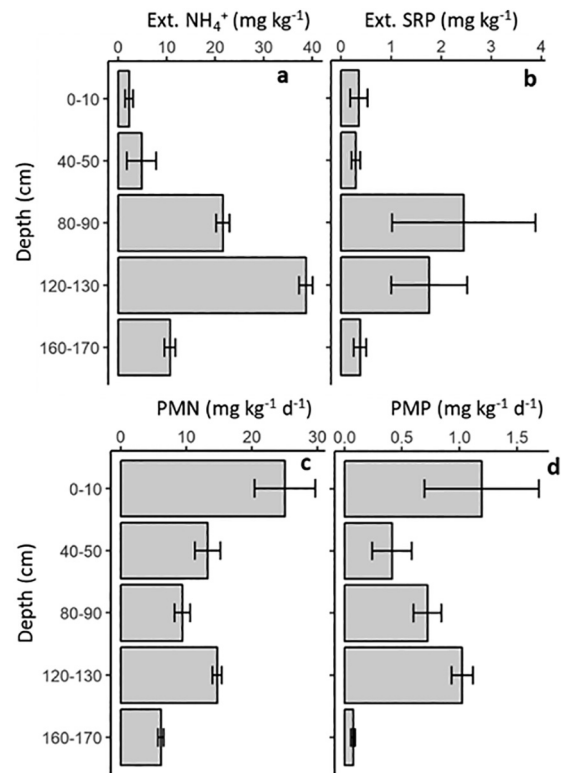


Fig. 6. Extractable NH_4^+ (Ext. NH_4^+), Extractable soluble reactive phosphorus (Ext. SRP) and Potentially Mineralizable Nitrogen (PMN) and Phosphorus (PMP) at some depths of eroding marsh edge soil. The data expressed as mean \pm standard error ($n = 3$).

analyzed (Supplementary Table 4). The extractable NH_4^+ was significantly lower ($p < 0.0001$) at the surface of the estuary bottom (0–10 cm) compared to deeper soil. There was no comparison of these biogeochemical properties with the marsh edge soil due to different depths analyzed for marsh edge and submerged soil.

3.5. ^{14}C dating of the organic matter

The calibrated radiocarbon age of the organic matter at the bottom of the estuary 34 m from the edge of the marsh was 386 ± 82 ybp and that of 58 m from the edge was 391 ± 82 ybp

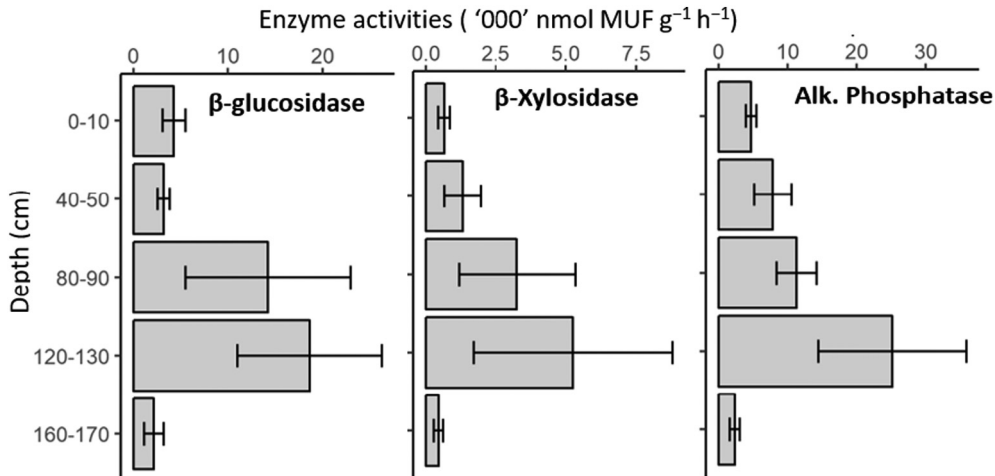


Fig. 5. Extracellular enzyme activities at some depths of eroding marsh edge soil. The data expressed as mean \pm standard error ($n = 3$).

([Table 1](#)). At present (2020 CE), mean age of the organic matter from estuary bottom (105–115 cm depth from marsh surface) was 458 ± 84 years with the long-term accretion rate of $2.4 \pm 0.5 \text{ mm yr}^{-1}$. The $\delta^{13}\text{C}$ values ranged from -18 to -25‰ .

4. Discussion

4.1. Vertical carbon profile and depositional environment

The total carbon content increased with depth both on concentration (g kg^{-1} soil) and volumetric (carbon density) basis confirming the large storage of carbon at depths in these coastal wetlands. Some other studies conducted in Barataria Basin, Louisiana have also shown increased carbon content up to the depth of 1 m ([Steinmuller et al., 2019](#); [Haywood et al., 2020](#)) and 1.5 m ([Steinmuller and Chambers, 2019](#)). Our finding confirms the increasing trends of soil carbon with depth in opposition of the well observed relationship of decreasing soil carbon with depth at other marsh sites ([Webster and Benfield, 1986](#); [Schipper and Reddy, 1995](#); [Mendelsohn et al., 1999](#); [Reddy and DeLaune, 2008](#)). The carbon stock assessments in wetland soil including blue carbon offset methodologies considers top one-meter soil depth to estimate the carbon storage ([Mack et al., 2012](#); [Howard et al., 2014](#); [Emmer et al., 2015](#); [Sapkota and White, 2020](#)). Our findings indicate a need for consideration of a deeper (>1 m) carbon profile and depositional environment for blue carbon stock assessments.

The increasing trend of total carbon up to a depth of 120–130 cm and fluctuation across the depth indicates hydrologic changes on a historical time scale. The hydrologic change is further corroborated by the variation in the bulk density across depth (Supplementary Fig. 1). The presence of the mud layer below the depth of the 180 cm indicate that there was a continuous supply of the sediment from the Mississippi River until this depth ([DeLaune et al., 2013](#); [Roberts et al., 2015](#)). The gradual accretion of organic matter above this depth of 180 cm indicate a reduction in the river sediment supply. This reduction in sediment supply may be related major hydrologic change in the Barataria Basin, likely the shift in the delta lobes of the Mississippi River. The establishment of wetlands above the depth of 180 cm and other small hydrologic changes is well supported by bulk density fluctuation (Supplementary Fig. 1) and the presence of an organic and inorganic form of phosphorus. Presence of high TOP and low TIP above the depth of the 160 cm is the indication of no river connection ([Fig. 4](#)) ([Spera et al., 2020](#)). During the early stage of development, these marshes may have been fresh to intermediate marshes with very little source of sediment as indicated by $\delta^{13}\text{C}$ values ([DeLaune, 1986](#)). In addition, the marshes were not fragmented providing the large accommodation space for vertical accretion. With sea-level rise and hydrologic changes, the carbon sequestered at depths, especially below the depth of 1 m, may have been buried and well preserved. With continuous global sea-level rise, subsidence, erosion, and fragmentation, these marshes gradually converted into brackish/salt marshes. Salt marshes lie at the elevation close to the sea-level and maybe a good indicator of the historical sea-level ([Kelsey, 2015](#)). Some geologic studies have used the radiocarbon dating of peat materials to understand the past sea-level in coastal Louisiana ([González and Törnqvist, 2009](#); [Wang et al., 2019](#)). Additional isotopic, sedimentary, and radiocarbon analysis may be essential to understand the

depositional environment of the vertical carbon profiles in Barataria Basin, Louisiana.

4.2. Molecular complexity of carbon and microbial activities

The results of carbon separation indicate the storage of a significant amount of labile pool of carbon at depth. The labile consists of 14–21% of TC and is consistent with the literature. Using a similar method, [Steinmuller and Chambers \(2019\)](#) found 17–30% of labile carbon while using a different methodology, [Dodla et al. \(2012\)](#) found 16–23% of labile carbon up to 175 cm deep in brackish marsh of Barataria Basin Louisiana. The labile pool of carbon has likely been preserved since burial for centuries under reduced soil conditions. In addition to this, a small amount of labile carbon may have been formed due to a very slow breakdown of more refractory organic matter. The decreasing proportion of labile carbon at depth indicates a slow breakdown of preserved labile carbon at depths. This decreasing proportion of labile carbon may also be related to the residence time of the carbon at different depths. The radiocarbon age of the carbon is increasing with depth as indicated by the results of this study and our previous study ([Sapkota and White, 2019](#)). Since these marshes lie in abandoned delta lobe of the Mississippi River, subsidence due to compaction and decomposition of the organic matter is common ([Nyman, 2014](#)).

The % OM was significantly lower at the surface of the estuary bottom than the corresponding depth of marsh edge soil indicating the mineralization of SOM at the aerobic zone of soil water interface ([Reddy and DeLaune, 2008](#)) and this similar conclusion was reached by [Haywood et al. \(2020\)](#) who examined the spectroscopic nature of the porewater dissolved organic carbon (DOC).

Microbes produce enzymes to breakdown complex carbon compounds into simpler compounds used as a source of energy or to release nutrients. The presence of enzyme activities at all depth of the marsh edge soil indicates the presence of microbial activity at depths. The increasing trend of the marsh edge soil enzyme activities with depth is indicated by their strong correlation with the TC, TN, % OM, and LPC; which all variably increased with depth. Likewise, the microbes break down organic carbon and release nutrients, e.g. inorganic form of nitrogen (NH_4^+) and phosphorus (SRP). The Ext. NH_4^+ and Ext. SRP concentration increased with depth. Few other studies in Barataria Basin reported increased Ext. NH_4^+ and Ext. SRP concentrations at depths ([Steinmuller et al., 2019](#); [Steinmuller and Chambers, 2019](#); [Steinmuller et al., 2020](#)). The PMN and PMP rates were highest at the surface and generally decreased with depth indicating more biological activity at the surface and root zone of the marshes. However, significant microbial activity is present at depths as indicated by the concentration of Ext. NH_4^+ , Ext. SRP, extracellular enzyme activities, and PMN and PMP rates. This finding is well supported by the presence of a substantial amount of labile carbon at all depths of the soil. The presence of significant labile carbon and microbial activities indicates the availability of “good quality” carbon for potential microbial degradation. [Steinmuller et al. \(2019\)](#), reported that the deeper soil produced 4 times greater CO_2 than the soil at the surface of the wetland indicating the presence of labile carbon and the microbial community at depths in a bottle incubation experiment that exposed wetland soil (100 cm deep) to aerobic condition. [Steinmuller and Chambers \(2019\)](#) found a

Table 1

Radiocarbon dating results of decayed plant materials from estuarine bottom. Samples collected on 01/27/2020. Laboratory code: Beta - Beta Analytic, Miami, FL, USA, Calibration used-BetaCal3.21: High Probability Density Range Method (HPD): INTCAL13, BP = Before Present (1950 CE).

GPS Coordinates	Distance from marsh edge (m)	Water depth (cm)	Depth from marsh surface (cm)	Lab Code	Fraction modern carbon	$\delta^{13}\text{C}$ (‰)	Conventional radiocarbon age (BP)	Calendar years (cal CE)	Calibrated radiocarbon age (ybp)
29.44657, -89.90633	34	87	105–115	Beta-551,765	0.9609 ± 0.0036	-18	320 ± 30	1482–1646	386 ± 82
29.44655, -89.90652	58	87	105–115	Beta-551,766	0.9598 ± 0.0036	-25.2	330 ± 30	1477–1642	391 ± 82

noticeable number of microbial gene copies across the entire depth (1.5 m) of soil analyzed.

The presence of the microbial activities at different depths of the submerged soil indicates that the SOM quality did not change with submergence except at the surface of the estuarine bottom. Upon release of this SOM into the water, mineralization is likely to occur.

4.3. Synthesis on fate of eroding carbon

It is essential to understand what happens when carbon moves from the physical mechanism of erosion to submergence and the ultimate fate of eroding carbon. The primary mechanism of erosion is due to undercutting below the root zone specifically when the wind waves strike below the surface of the marsh (Sapkota and White, 2019; Valentine and Mariotti, 2019). Initially, the organic matter present in or below the root zone, approximately 20–40 cm depth, is exposed to well oxygenated surface water and high energy at the estuarine edge of the marsh. The marsh soil then undergoes slumping of the hanging structures (surface and root zone) and results in the release of the additional organic matter and plant parts (root and shoot) into the bay. As indicated by the result of PMN, PMP, and enzyme activities this zone had some of the highest microbial activity. Continuous agitations of the shallow bay water by wind waves maintain the well oxygenated water column. The availability of oxygen as an electron acceptor is highly favored by the microbes, increasing the mineralization of organic matter up to 6 times compared to anaerobic conditions (Bridgman et al., 1998; Reddy and DeLaune, 2008). The labile pool of carbon becomes oxidized quickly with the energetically favored electron acceptor, oxygen, in high supply. The plant parts including shoots, live and dead roots, and other organic matter may be consumed by the aquatic macrofauna and released as simpler forms of the carbon through excretion into the bay. The microbes could potentially mineralize the carbon present in the macrofauna's excreta (Wotton and Malmquist, 2001).

As described above, the initial depth of the erosion is approximately 40 cm. Due to continuous action of the wind waves, the bay achieves an equilibrium depth profile of approximately 1.5 m (Wilson and Allison, 2008; Sapkota and White, 2019). During this process, continuous scouring of the recently eroded submerged sloping bottom of the estuary will occur over the course of time. The slow but continuous release of the stored organic matter into aerobic estuarine water takes place. This portion of soil has substantial microbial activities as evidenced by the results of PMN, PMP, bioavailable nutrients, and enzyme activities. Upon exposure to the aerobic water column of the estuary, the labile pool of carbon gets mineralized quickly. This indicates that up to 21% of the eroded SOM (i.e. labile portion) gets mineralized in a short period of time. The remaining almost 79% of the SOM is relatively refractory and may take a longer time to degrade into simpler forms. Oxygen availability is required for phenol oxidase to degrade the more recalcitrant carbon compounds. The decomposition of SOM under the aerobic water of the estuary is a continuous process as evidenced by the presence of microbial activity in the entire depth of the soil. However, it is still unclear on the proportion of the eroded SOM mineralized in the coastal estuaries. Besides mineralization in the bay, a portion of the carbon could potentially be reburied on the bay bottom (Li et al., 2009; Macreadie et al., 2013), transport to the coastal ocean (Bianchi et al., 2008; Li et al., 2009) or transported back to the marsh surface by waves (Hopkinson et al., 2018; Mariotti et al., 2020).

The radiocarbon age (388 ± 84 ybp) of intact peat layer just below shell hash in the estuarine bottom was consistent with the age of the carbon at similar depths in marshes of Barataria Basin (Sapkota and White, 2019; Bomer et al., 2019). Sapkota and White (2019) found that the age of the organic matter at the depth of 150–160 cm in the marshes close to our sampling points was 781 ± 111 ybp with long term accretion rate of 2.0 ± 0.3 mm yr $^{-1}$. Bomer et al. (2019) estimated the age of the peat at the depth of 60–61 cm to be 235 ± 132 ybp with long-term accretion rate of 3.7 ± 2.1 mm yr $^{-1}$ from the sites

approximately 20 km northwest of our study sites. The $\delta^{13}\text{C}$ values (Table 1) indicate the existence of intermediate marshes (DeLaune, 1986; Chmura et al., 1987) before 388 ± 84 ybp in the northern part of Barataria Bay, which are now *Spartina alterniflora* dominated brackish/salt marshes at the surface.

There was non-deposition above a layer of older peat in the estuarine bottom. This age of peat material also indicates that there is no reburial of the eroded relatively young organic matter at the estuarine bottom. Vaccare et al. (2019) found a thin mud layer over a layer of intact peat on the estuarine bottom at various distance from the edge of the marsh indicating that the eroded carbon is not being buried on the estuarine bottom. In addition, there is no artifact of the marsh (e.g. pieces of roots) on the bottom of the bay. The high bulk density and low organic matter content of the bay sediment also indicate that the eroded carbon is not reburied in the estuarine bottom (White et al., 2009; Pietroski et al., 2015; Vaccare et al., 2019). Likewise, the majority of the organic carbon present in coastal bays sediment is derived from phytoplankton rather than from salt marsh plants (DeLaune and Lindau, 1987).

Valentine and Mariotti (2019) indicated that erosion occurs when the wave height is at or below the surface of the marsh. During the over-shooting of the waves over the marsh, erosion is less indicating a very small amount of the organic matter transport back into the marsh. However, due to the continuous scouring on the submerged part of the estuary, some amount of SOM and sediment may be transported back onto the surface of the marsh (Hopkinson et al., 2018). However, during the drainage of the marsh surface, the organic matter may be easily mobilized and transported away. Likewise, upon drainage, the settled organic matter on marsh surface can also be easily mineralized.

The estuarine area (approx. 456 km 2) is relatively larger than eroding area of adjacent marsh. Thus, the eroded SOM has a relatively long residence time of approximately 150 days in the aerobic estuarine surface water providing ample opportunity for mineralization (Solis and Powell, 1999). Sampere et al. (2008) through the study of lignin and pigment markers in the surface sediment of the Louisiana continental margin indicated that the carbon input from coastal wetlands and bay were likely rapidly decomposed and not preserved. This collection of disparate studies indicates a high likelihood that the eroded carbon is mineralized in the estuary and emitted back into the atmosphere as CO₂ or present in the water column as DOC on very low concentrations (Haywood et al., 2020).

4.4. Ecosystem and global implications

Our study and evidence from the literature indicate that the vast majority of SOM eroded by marsh edge erosion is mineralized to CO₂. Studies in our research sites have shown that over the course of time, the depth of marsh organic platform erosion could be up to 1.5 m (Wilson and Allison, 2008; Sapkota and White, 2019). This depth corresponds to the storage of a large amount of soil carbon (189,000 ton CO₂ e km $^{-2}$) which eventually is eroded and mineralized (Fig. 3b). The storage of carbon below this depth rapidly declines indicating that only a small portion of the original coastal wetland soil carbon is more permanently preserved after edge erosion induced loss. As a result, the erosional perimeters of the marshes in wetland-dominated coastlines are turning into a net source of CO₂ emission through the loss of annual sequestration and the centuries of exhumed and mineralized organic soil C (Holmquist et al., 2018).

In addition to CO₂ emission, the edge erosion results in the release of a large amount of the stored NH₄⁺ and SRP into the adjacent estuary (Steinmuller et al., 2020). The mineralization of the organic matter also releases NH₄⁺ and SRP (Bridgman et al., 1998; Reddy and DeLaune, 2008). These inorganic forms of N and P could potentially contribute to the existing nutrient pollution in coastal estuaries and hypoxia on the continental shelf (Bianchi et al., 2008; Steinmuller et al., 2020).

Conservatively assuming 75% mineralization of the eroded carbon, the carbon emission from Barataria Basin, Louisiana and the all of coastal Louisiana is 1.8×10^6 ton CO₂ e yr $^{-1}$ and 8.1×10^6 ton CO₂ e yr $^{-1}$

respectively (Table 2). Globally, the carbon emission from coastal wetland loss is $431.2 * 10^6$ ton CO₂ e yr⁻¹ (Table 2). Our study was conducted in a coastal basin experiencing high relative rates of sea-level rise (~13 mm yr⁻¹) that other more stable coastlines across the globe are projected to experience in the next 50–60 years (Horton et al., 2014; Jankowski et al., 2017). Results of this study can be taken as the proxy for the fate of other wetland-dominated coastline that will be impacted by the sea-level rise in the near future. Globally, coastal wetlands sequester almost $700 * 10^6$ ton CO₂ e yr⁻¹ or a carbon sequestration rate of 800 ton CO₂ e km⁻² yr⁻¹ on an area basis (Murray et al., 2011). So far, coastal wetlands are a sink for atmospheric carbon. However, these wetlands may become net sources of carbon if current trends of coastal wetland loss continues with rising sea-level. Efforts to protect coastal wetlands from erosive land loss should be implemented before it is too late to reduce CO₂ emission from the coastal ecosystem due to edge erosion.

5. Conclusion

The quantity, molecular complexity and biogeochemical properties of the soil organic matter in eroding and submerged coastal wetland soil were studied along a subsiding coastal margin. These results can be used to predict the fate of coastal wetland SOM along more stable coastlines in the near future under increasing rates of sea-level rise. The percent organic matter, total carbon, labile carbon, and bioavailable nutrients increased with depth down to 1.3 m. The increasing carbon content with depth indicates that blue carbon stock assessment should consider deeper carbon profiles, e.g. up to 2 m. Higher TOP compared with TIP can also be taken as an indicator of wetland development and separation from river in the deltaic system. In addition, the microbial activity was present across all depths of the soils studied. Upon exposure of this good quality organic matter to the aerobic water column of the estuary, the SOM is mineralized to CO₂ and emitted back to the atmosphere. This mineralization is enhanced by the maintenance of the aerobic water column due to the continuous aeration of the shallow estuarine water by wind waves. The old radiocarbon dates of estuarine bottom SOM and evidence from the literature indicate that the eroded carbon is neither reburied in the estuarine sediment nor likely gets transported to the coastal ocean in particulate form. Additional work is essential to determine the relative portion of the SOM mineralized vs transported back to the marsh platform and coastal ocean as DOC. The CO₂ emission from marsh edge erosion induced SOM loss may contribute to the ever-increasing atmospheric CO₂ concentrations. The coastal marshes experiencing high relative sea-level rise at present (e.g. coastal LA) are already losing the large storage of blue carbon through marsh edge erosion. The other stable wetland-dominated coastlines across the globe may experience similar wetland carbon loss in the near future as the eustatic sea-level rises to reach the level of relative sea-level rise in coastal Louisiana unless efforts are undertaken to stabilize these marshes.

CRedit authorship contribution statement

Yadav Sapkota: Conceptualization, Investigation, Methodology, Writing - original draft. **John R. White:** Writing - review & editing, Supervision, Funding acquisition.

Table 2

Carbon emission from coastal wetland loss conservatively assuming the mineralization of 75% of eroded carbon. Wetland area and annual loss in Louisiana was taken from Couvillion et al. (2017). The Global wetland area and annual loss was taken from Davidson (2014) and Davidson et al. (2018). The carbon stock (1.5 m deep) for Louisiana was calculated from this study. The global carbon stock (1 m deep) was taken from Murray et al. (2011).

Coastal wetlands	Area (km ²)	Wetland loss (km ² yr ⁻¹)	Carbon stock (tCO ₂ e km ⁻²)	Annual CO ₂ emission (t CO ₂ e yr ⁻¹)
Barataria Basin, Louisiana	2712	13.3	189,000	$1.8 * 10^6$
Coastal Louisiana	14,710	57.5	189,000	$8.1 * 10^6$
Global stock	660,000	6270	91,700	$431.2 * 10^6$

Declaration of competing interest

The authors declare that they have no known competing financial interests or personal relationships that could have appeared to influence the work reported in this paper.

Acknowledgements

This work was funded under a collaborative National Science Foundation Chemical Oceanography Grant (#1636052). Y. Sapkota was funded by an Economic Development Assistantship from the Graduate School, Louisiana State University. We also acknowledge Peter T. Mates, Michael P. Hayes, and Eddie Weeks for help with fieldwork and Havalend Steinmuller for laboratory assistance.

Appendix A. Supplementary data

Supplementary data to this article can be found online at <https://doi.org/10.1016/j.scitotenv.2020.141913>.

References

Andersen, J.M., 1976. An ignition method for determination of total phosphorus in lake sediments. *Water Res.* 10, 329–331. [https://doi.org/10.1016/0043-1354\(76\)90175-5](https://doi.org/10.1016/0043-1354(76)90175-5).

Bianchi, T.S., Canuel, E.A., 2011. *Chemical Biomarkers in Aquatic Ecosystems*. Princeton University Press.

Bianchi, T.S., Dimarco, S.F., Allison, M.A., Chapman, P., Cowan, J.H., Hetland, R.D., Morse, J.W., Rowe, G., 2008. Controlling hypoxia on the U.S. Louisiana Shelf: beyond the nutrient-centric view. *EOS Trans. Am. Geophys. Union* 89, 236–237. <https://doi.org/10.1029/2008EO260005>.

Blum, M.D., Roberts, H.H., 2009. Drowning of the Mississippi Delta due to insufficient sediment supply and global sea-levelrise. *Nat. Geosci.* 2 (7), 488–491. <https://doi.org/10.1038/ngeo553>.

Bomer, E.J., Bentley, S.J., Hughes, J.E.T., Wilson, C.A., Crawford, F., Xu, K., 2019. Deltaic morphodynamics and stratigraphic evolution of Middle Barataria Bay and Middle Breton Sound regions, Louisiana, USA: implications for river-sediment diversions. *Estuar. Coast. Shelf Sci.* 224 (March), 20–33. <https://doi.org/10.1016/j.ecss.2019.03.017>.

Bridgeman, S.D., Updegraff, K., Pastor, J., 1998. Carbon, nitrogen, and phosphorus mineralization in northern wetlands. *Ecology* 79 (5), 1545–1561. [https://doi.org/10.1890/0012-9658\(1998\)079\[1545:CNAPMI\]2.0.CO;2](https://doi.org/10.1890/0012-9658(1998)079[1545:CNAPMI]2.0.CO;2).

Bronk Ramsey, C., 2009. Bayesian analysis of radiocarbon dates. *Radiocarbon* 51 (1), 337–360. <https://doi.org/10.1017/S0033822200033865>.

Chmura, G., Aharon, P., Socki, R., Abernethy, R., 1987. An inventory of ¹³C abundances in coastal wetlands of Louisiana, USA: vegetation and sediments. *Oecologia* 74, 264–271.

Chmura, G.L., Anisfeld, S.C., Cahoon, D.R., Lynch, J.C., 2003. Global carbon sequestration in tidal, saline wetland soils. *Glob. Biogeochem. Cycles* 17. <https://doi.org/10.1029/2002gb001917>.

Choi, Y., Wang, Y., 2004. Dynamics of carbon sequestration in a coastal wetland using radiocarbon measurements. *Glob. Biogeochem. Cycles* 18, 1–12. <https://doi.org/10.1029/2004GB002261>.

Couvillion, B.R., Beck, H., Schoolmaster, D., Fischer, M., 2017. Land area change in coastal Louisiana (1932 to 2016) scientific investigations map 3381. U.S. Geological Survey Scientific Investigations Map 3381, p. 16 <https://doi.org/10.3133/SIM3381>.

Davidson, N.C., 2014. How much wetland has the world lost? Long-term and recent trends in global wetland area. *Mar. Freshw. Res.* 65 (10), 934–941. <https://doi.org/10.1071/MF14173>.

Davidson, N.C., Fluet-Chouinard, E., Finlayson, C.M., 2018. Global extent and distribution of wetlands: trends and issues. *Mar. Freshw. Res.* 69 (4), 620–627. <https://doi.org/10.1071/MF17019>.

DeBusk, W.F., Reddy, K.R., 1998. Turnover of detrital organic carbon in a nutrient-impacted Everglades marsh. *Soil Sci. Soc. Am. J.* 62, 1460–1468.

DeLaune, R.D., 1986. The use of $\delta^{13}\text{C}$ signature of C-3 and C-4 plants in determining past depositional environments in rapidly accreting marshes of the Mississippi River deltaic plain, Louisiana, U.S.A. *Chem. Geol. Isot. Geosci. Sect.* 59 (C), 315–320. [https://doi.org/10.1016/0168-9622\(86\)90080-1](https://doi.org/10.1016/0168-9622(86)90080-1).

DeLaune, R.D., Lindau, C.W., 1987. $\delta^{13}\text{C}$ signature of organic carbon in estuarine bottom sediment as an indicator of carbon export from adjacent marshes. *Biogeochemistry* 4 (3), 225–230. <https://doi.org/10.1007/BF02187368>.

DeLaune, R.D., White, J.R., 2012. Will coastal wetlands continue to sequester carbon in response to an increase in global sea level?: a case study of the rapidly subsiding Mississippi river deltaic plain. *Clim. Chang.* 110 (1–2), 297–314. <https://doi.org/10.1007/s10584-011-0089-6>.

DeLaune, R.D., Kongchum, M., White, J.R., Jgsujinda, A., 2013. Freshwater diversions as an ecosystem management tool for maintaining soil organic matter accretion in coastal marshes. *Catena* 107, 139–144. <https://doi.org/10.1016/j.catena.2013.02.012>.

Dodla, S.K., Wang, J.J., DeLaune, R.D., 2012. Characterization of labile organic carbon in coastal wetland soils of the Mississippi River deltaic plain: relationships to carbon functionalities. *Sci. Total Environ.* 435–436, 151–158. <https://doi.org/10.1016/j.scitotenv.2012.06.090>.

Emmer, I., Needelman, B., Emmett-Mattox, S., Crooks, S., Megonigal, P., Myers, D., Oreska, M., McGlathery, K., Shoch, D., 2015. *VM0033 Methodology for TidalWetland and Seagrass Restoration V1.0. Verified Carbon Standard (VCS)*, Washington, DC.

Flint, R., Deevey, E.S., 1962. Editorial Statement. *Radiocarbon* 4 (i–ii).

Georgiou, I.V., FitzGerald, D.M., Stoney, G.W., 2005. *The impact of physical processes along the Louisiana coast*. *J. Coast. Res.* 44, 72–89.

German, D.P., Weintraub, M.N., Grandy, A.S., Lauber, C.L., Rinkes, Z.L., Allison, S.D., 2011. Optimization of hydrolytic and oxidative enzyme methods for ecosystem studies. *Soil Biol. Biochem.* 43 (7), 1387–1397. <https://doi.org/10.1016/j.soilbio.2011.03.017>.

González, J.L., Törnqvist, T.E., 2009. A new Late Holocene sea-level record from the Mississippi Delta: evidence for a climate/sea level connection? *Quat. Sci. Rev.* 28 (17–18), 1737–1749. <https://doi.org/10.1016/j.quascirev.2009.04.003>.

Haywood, B.J., Hayes, M.P., White, J.R., Cook, R.L., 2020. Potential fate of wetland soil carbon in a deltaic coastal wetland subjected to high relative sea level rise. *Sci. Total Environ.*, 135185. <https://doi.org/10.1016/j.scitotenv.2019.135185>.

Hinson, A.L., Feagin, R.A., Eriksson, M., 2019. Environmental controls on the distribution of tidal wetland soil organic carbon in the continental United States. *Glob. Biogeochem. Cycles* 33, 1408–1422. <https://doi.org/10.1029/2019GB006179>.

Holmquist, J., Windham-Myers, L., Bernal, B., Byrd, K.B., Crooks, S., Gonanea, M.E., et al., 2018. Uncertainty in United States coastal wetland greenhouse gas inventorying. *Environ. Res. Lett.* 13 (11), 115005. <https://doi.org/10.1088/1748-9326/aae157>.

Hopkinson, C.S., Morris, J.T., Fagherazzi, S., Wollheim, W.M., Raymond, P.A., 2018. Lateral marsh edge erosion as a source of sediments for vertical marsh accretion. *J. Geophys. Res. Biogeosci.* 123 (8), 2444–2465. <https://doi.org/10.1029/2017JG004358>.

Horton, B.P., Rahmstorf, S., Engelhart, S.E., Kemp, A.C., 2014. Expert assessment of sea-level rise by AD 2100 and AD 2300. *Quat. Sci. Rev.* 84, 1–6. <https://doi.org/10.1016/j.quascirev.2013.11.002>.

Howard, J., Hoyt, S., Isensee, K., Pidgeon, E., Telszewski, M. (Eds.), 2014. *Coastal Blue Carbon: Methods for Assessing Carbon Stocks and Emissions Factors in Mangroves, Tidal Salt Marshes, and Seagrass Meadows*. Conservation International, Intergovernmental Oceanographic Commission of UNESCO, International Union for Conservation of Nature, Arlington, Virginia, USA.

Jankowski, K.L., Tornqvist, T.E., Fernandes, A.M., 2017. Vulnerability of Louisiana's coastal wetlands to present-day rates of relative sea-level rise. *Nat. Commun.* 8 (14792), 1–7. <https://doi.org/10.1038/ncomms14792>.

Kelsey, R.G., 2015. *Geomorphological indicators of past sea levels*. In: Shennan, I., Long, A.J., Horton, B.P. (Eds.), *Handbook of Sea-level Research*. John Wiley & Sons, Ltd, West Sussex, UK.

Levine, B.M., White, J.R., DeLaune, R.D., 2017. Impacts of the long-term presence of buried crude oil on salt marsh soil denitrification in Barataria Bay, Louisiana. *Ecol. Eng.* 99, 454–461. <https://doi.org/10.1016/j.ecoleng.2016.11.017>.

Li, C., Swenson, E., Weeks, E., White, J.R., 2009. Asymmetric tidal straining across an inlet: lateral inversion and variability over a tidal cycle. *Estuar. Coast. Shelf Sci.* 85 (4), 651–660. <https://doi.org/10.1016/j.ecss.2009.09.015>.

Mack, S.K., Lane, R.R., Day, J.W., 2012. *Restoration of Degraded Deltaic Wetland of the Mississippi Delta*. American Carbon Registry, Arlington VA.

Macreadie, P.I., Hughes, A.R., Kimbro, D.L., 2013. Loss of 'blue carbon' from coastal salt marshes following habitat disturbance. *PLoS One* 8, e69244.

Macreadie, P.I., Anton, A., Raven, J.A., Beaumont, N., Connolly, R.M., Friess, D.A., et al., 2019. The future of blue carbon science. *Nat. Commun.* 10 (1), 1–13. <https://doi.org/10.1038/s41467-019-11693-w>.

Mariotti, G., Bruno, G., Valentine, K., 2020. Mud-associated organic matter and its direct and indirect role in marsh organic matter accumulation and vertical accretion. *Limnol. Oceanogr.* 1–15 <https://doi.org/10.1002/lo.11475>.

Mendelsohn, I.A., Sorrell, B.K., Brix, H., Schierup, H.H., Lorenzen, B., Maltby, E., 1999. Controls on soil cellulose decomposition along a salinity gradient in a *Phragmites australis* wetland in Denmark. *Aquat. Bot.* 64 (3–4), 381–398. [https://doi.org/10.1016/S0304-3770\(99\)00065-0](https://doi.org/10.1016/S0304-3770(99)00065-0).

Morton, R.A., Bernier, J.C., Kelso, K.W., 2009. Recent subsidence and erosion at diverse wetland sites in the southeastern Mississippi Delta Plain. *US Geological Series Open File Report*, vol. 2009–1158.

Murray, B.C., Pendleton, L., Jenkins, W.A., Sifleet, S., 2011. *Green Payments for Blue Carbon: Economic Incentives for Protecting Threatened Coastal Habitats*. 52 pp. Nicholas Institute for Environmental Policy Solutions, Duke University, Durham, NC.

Nahluk, A.M., Fennessy, M.S., 2016. Carbon storage in US wetlands. *Nat. Commun.* 7, 1–9. <https://doi.org/10.1038/ncomms13835>.

Needelman, B.A., Emmer, I.M., Emmett-Mattox, S., Crooks, S., Megonigal, J.P., Myers, D., et al., 2018. The science and policy of the verified carbon standard methodology for tidal wetland and seagrass restoration. *Estuar. Coasts* 41 (8), 2159–2171. <https://doi.org/10.1007/s12237-018-0429-0>.

NOAA, 2019. NOAA research news. Available at: <https://research.noaa.gov/article/ArtMID/587/ArticleID/2461/Carbon-dioxide-levels-hit-peak-in-May>. (Accessed 20 August 2019).

Nyman, J.A., 2014. Integrating successional ecology and the delta lobe cycle in wetland research and restoration. *Estuar. Coasts* 37 (6), 1490–1505. <https://doi.org/10.1007/s12237-013-9747-4>.

Nyman, J.A., Carlsson, M., DeLaune, R.D., Patrick, H., 1994. Erosion rather than plant dieback as the mechanism of marsh loss in a estuarine marsh. *Earth Surf. Process. Landf.* 19, 69–84.

Oades, J.M., Kirkman, M.A., Wagner, G.H., 1970. The use of gas-liquid chromatography for the determination of sugars extracted from soils by sulfuric acid. *Soil Sci. Soc. Am. J.* 34, 230–235. <https://doi.org/10.2136/sssaj1970.03615995003400020017x>.

Pietroski, J.P., White, J.R., DeLaune, R.D., Wang, J.J., Dodla, S.K., 2015. Fresh and weathered crude oil effects on potential denitrification rates of coastal marsh soil. *Chemosphere* 134, 120–126. <https://doi.org/10.1016/j.chemosphere.2015.03.056>.

Qualls, R.G., 2013. Dissolved organic matter. In: DeLaune, R.D., Reddy, K.R., Richardson, C.J., Megonigal, J.P. (Eds.), *Methods in Biogeochemistry of Wetlands*. Soil Science Society of America, Inc, Madison, Wisconsin, USA.

Reddy, K.R., DeLaune, R.D., 2008. *Biogeochemistry of Wetlands: Science and Applications*. CRC Press.

Reimer, P.J., Bard, E., Bayliss, A., Beck, J.W., Blackwell, P.G., Bronk, C., Caitlin, R., Hai, E.B., Edwards, R.L., et al., 2013. *Intcal13 and marine13 radiocarbon age calibration curves 0–50,000 years cal bp*. *Radiocarbon* 55, 1869–1887.

Richardson, C.J., Reddy, K.R., 2013. Phosphorus characterization and analysis of wetland soils. In: DeLaune, R.D., Reddy, K.R., Richardson, C.J., Megonigal, J.P. (Eds.), *Methods in Biogeochemistry of Wetlands*. Soil Science Society of America, Inc, Madison, Wisconsin, USA.

Roberts, H.H., DeLaune, R.D., White, J.R., Li, C., Sasser, E., Braud, D., Weeks, E., Khalid, S., 2015. Floods and cold front passages: impacts on coastal marshes in a river diversion setting (Wax Lake Delta, Louisiana). *J. Coast. Res.* 31 (5), 1057–1068. <https://doi.org/10.2112/COASTRES-D-14-00173.1>.

Rovira, P., Vallejo, V.R., 2002. Labile and recalcitrant pools of carbon and nitrogen in organic matter decomposing at different depths in soil: an acid hydrolysis approach. *Geoderma* 107 (1–2), 109–141. [https://doi.org/10.1016/S0016-7061\(01\)00143-4](https://doi.org/10.1016/S0016-7061(01)00143-4).

Sampere, T.P., Bianchi, T.S., Wakeham, S.G., Allison, M.A., 2008. Sources of organic matter in surface sediments of the Louisiana continental margin: effects of major depositional/transport pathways and hurricane Ivan. *Cont. Shelf Res.* 28 (17), 2472–2487. <https://doi.org/10.1016/j.csr.2008.06.009>.

Sapkota, Y., White, J.R., 2019. Marsh edge erosion and associated carbon dynamics in coastal Louisiana: a proxy for future wetland-dominated coastlines world-wide. *Estuar. Coast. Shelf Sci.* 226. <https://doi.org/10.1016/j.ecss.2019.106289>.

Sapkota, Y., White, J.R., 2020. Carbon offset market methodologies applicable for coastal wetland restoration and conservation in the United States: a review. *Sci. Total Environ.* 701, 134497. <https://doi.org/10.1016/j.scitotenv.2019.134497>.

Schipper, L.A., Reddy, R.R., 1995. In situ determination of detrital breakdown in wetland soil-floodwater profile. *Soil Sci. Soc. Am. J.* 1437, 565–568. <https://doi.org/10.2136/sssaj1995.03615995005900020042x>.

Schmidt, M.W.J., Torn, M.S., Abiven, S., Dittmar, T., Guggenberger, G., Janssens, I.A., et al., 2011. Persistence of soil organic matter as an ecosystem property. *Nature* 478 (7367), 49–56. <https://doi.org/10.1038/nature10386>.

Sierra, C.A., Hoyt, A.M., He, Y., Trumbore, S.E., 2018. Soil organic matter persistence as a stochastic process: age and transit time distributions of carbon in soils. *Glob. Biogeochem. Cycles* 32, 1574–1588. <https://doi.org/10.1029/2018GB005950>.

Solis, R.S., Powell, G.L., 1999. *Hydrography, mixing characteristics, and residence times of Gulf of Mexico estuaries*. In: Bianchi, T.S., Pennock, J.R., Twilley, R.R. (Eds.), *Biogeochemistry of Gulf of Mexico Estuaries*. John Wiley and Sons, New York, pp. 29–71.

Sparks, D. (Ed.), 1996. *Methods of Soil Analysis. Part 3. Chemical Methods*. vol. 5. Soil Science Society of America, Inc, Madison, Wisconsin, USA.

Spera, A.C., White, J.R., Corstanje, R., 2020. Spatial and temporal changes to a hydrologically-reconnected coastal wetland: implications for restoration. *Estuar. Coast. Shelf Sci.* 238 (August 2019), 106728. <https://doi.org/10.1016/j.ecss.2020.106728>.

Steinmuller, H.E., Chambers, L.G., 2019. Characterization of coastal wetland soil organic matter: implications for wetland submergence. *Sci. Total Environ.* 677, 648–659. <https://doi.org/10.1016/j.scitotenv.2019.04.405>.

Steinmuller, H.E., Dittmar, K.M., White, J.R., Chambers, L.G., 2019. Understanding the fate of soil organic matter in submerging coastal wetland soils: a microcosm approach. *Geoderma* <https://doi.org/10.1016/j.geoderma.2018.08.020> (December 2017).

Steinmuller, H.E., Hayes, M.P., Hurst, N.R., Sapkota, Y., Cook, R.L., White, J.R., et al., 2020. Does edge erosion alter coastal wetland soil properties? A multi-method biogeochemical study. *Catena* 187 (August 2019), 104373. <https://doi.org/10.1016/j.catena.2019.104373>.

USEPA, 1993. *Methods for Determination of Inorganic Substances in Environmental Samples*. PA/600/R-93/100. United States Environmental Protection Agency, Washington D.C.

Vaccare, J., Meselhe, E., White, J.R., 2019. The denitrification potential of eroding wetlands in Barataria Bay, LA, USA: implications for river reconnection. *Sci. Total Environ.* 686, 529–537. <https://doi.org/10.1016/j.scitotenv.2019.05.475>.

Valentine, K., Mariotti, G., 2019. Wind-driven water level fluctuations drive marsh edge erosion variability in microtidal coastal bays. *Cont. Shelf Res.* 176 (February), 76–89. <https://doi.org/10.1016/j.csr.2019.03.002>.

Vaughn, D.R., Bianchi, T.S., Shields, M.R., Kenney, W.F., Osborne, T.Z., 2020. Increased organic carbon burial in northern Florida mangrove-salt marsh transition zones. *Glob. Biogeochem. Cycles* 34, 1–21. <https://doi.org/10.1029/2019gb006334>.

Wang, J., Xu, K., Bentley, S.J., White, C., Zhang, X., Liu, H., 2019. Degradation of the plaquemines sub-delta and relative sea-level in eastern Mississippi deltaic coast

during late holocene. *Estuar. Coast. Shelf Sci.* 227 (August), 106344. <https://doi.org/10.1016/j.ecss.2019.106344>.

Webster, J.R., Benfield, E., 1986. *Vascular plant breakdown in freshwater ecosystems*. *Annu. Rev. Ecol. Syst.* 17, 67–94.

White, J.R., Reddy, K.R., 2000. Influence of phosphorus loading on organic nitrogen mineralization of Everglades soils. *Soil Sci. Soc. Am. J.* 64, 1525–1534. <https://doi.org/10.2136/sssaj2000.6441525x>.

White, J.R., Delaune, R.D., Li, C.Y., Bentley, S.J., 2009. Sediment methyl and total mercury concentrations along the Georgia and Louisiana inner shelf, USA. *Anal. Lett.* 42 (8), 1219–1231. <https://doi.org/10.1080/00032710902901947>.

Wickham, H., 2016. *ggplot2: Elegant Graphics for Data Analysis*. Springer-Verlag, New York.

Wilson, C.A., Allison, M.A., 2008. An equilibrium profile model for retreating marsh shorelines in southeast Louisiana. *Estuar. Coast. Shelf Sci.* 80, 483–494. <https://doi.org/10.1016/j.ecss.2008.09.004>.

Wood, S.E., White, J.R., Armbruster, C.K., 2017. Microbial processes linked to soil organic matter in a restored and natural coastal wetland in Barataria Bay, Louisiana. *Ecol. Eng.* 106, 507–514. <https://doi.org/10.1016/j.ecoleng.2017.06.028>.

Wotton, R.S., Malmquist, B., 2001. Feces in aquatic ecosystems. *BioScience* 51 (7), 537. [https://doi.org/10.1641/0006-3568\(2001\)051\[0537:fiae\]2.0.co;2](https://doi.org/10.1641/0006-3568(2001)051[0537:fiae]2.0.co;2).